



ARL-TR-8972 • JUNE 2020



# Simulations Predicting the Effects of Detonation Velocity on the Speed and Temperature of Shaped Charge Jets

by Robert Doney

Approved for public release; distribution is unlimited.

## **NOTICES**

### **Disclaimers**

The findings in this report are not to be construed as an official Department of the Army position unless so designated by other authorized documents.

Citation of manufacturer's or trade names does not constitute an official endorsement or approval of the use thereof.

Destroy this report when it is no longer needed. Do not return it to the originator.



# **Simulations Predicting the Effects of Detonation Velocity on the Speed and Temperature of Shaped Charge Jets**

**by Robert Doney**

*Weapons and Materials Research Directorate, CCDC Army Research Laboratory*

## REPORT DOCUMENTATION PAGE

*Form Approved*  
**OMB No. 0704-0188**

Public reporting burden for this collection of information is estimated to average 1 hour per response, including the time for reviewing instructions, searching existing data sources, gathering and maintaining the data needed, and completing and reviewing the collection information. Send comments regarding this burden estimate or any other aspect of this collection of information, including suggestions for reducing the burden, to Department of Defense, Washington Headquarters Services, Directorate for Information Operations and Reports (0704-0188), 1215 Jefferson Davis Highway, Suite 1204, Arlington, VA 22202-4302. Respondents should be aware that notwithstanding any other provision of law, no person shall be subject to any penalty for failing to comply with a collection of information if it does not display a currently valid OMB control number.

**PLEASE DO NOT RETURN YOUR FORM TO THE ABOVE ADDRESS.**

<b>1. REPORT DATE (DD-MM-YYYY)</b> June 2020		<b>2. REPORT TYPE</b> Technical Report		<b>3. DATES COVERED (From - To)</b> March 2019-May 2020	
<b>4. TITLE AND SUBTITLE</b> Simulations Predicting the Effects of Detonation Velocity on the Speed and Temperature of Shaped Charge Jets				<b>5a. CONTRACT NUMBER</b>	
				<b>5b. GRANT NUMBER</b>	
				<b>5c. PROGRAM ELEMENT NUMBER</b>	
<b>6. AUTHOR(S)</b> Robert Doney				<b>5d. PROJECT NUMBER</b> AH80	
				<b>5e. TASK NUMBER</b>	
				<b>5f. WORK UNIT NUMBER</b>	
<b>7. PERFORMING ORGANIZATION NAME(S) AND ADDRESS(ES)</b> US Army Combat Capabilities Development Command Army Research Laboratory ATTN: FCDD-RLW-PD Aberdeen Proving Ground, MD 21005-5066				<b>8. PERFORMING ORGANIZATION REPORT NUMBER</b> ARL-TR-8972	
<b>9. SPONSORING/MONITORING AGENCY NAME(S) AND ADDRESS(ES)</b>				<b>10. SPONSOR/MONITOR'S ACRONYM(S)</b>	
				<b>11. SPONSOR/MONITOR'S REPORT NUMBER(S)</b>	
<b>12. DISTRIBUTION/AVAILABILITY STATEMENT</b> Approved for public release; distribution is unlimited.					
<b>13. SUPPLEMENTARY NOTES</b> primary author's email: <robert.L.doney4.civ@mail.mil>.					
<b>14. ABSTRACT</b> In this report, I evaluate the effects of a warhead's detonation velocity on the resulting speed and thermodynamic state of shaped charge jets using the multiphysics code, ALEGRA. Specifically, I investigate a 65-mm, bare, shaped charge jet, generated from explosives that feature detonation velocities ranging from 6.84 to 9.11 km/s with a fixed geometry. Data showed a general trend for all cases: a hot axis that cools off with increasing radius according to a second-order polynomial. At higher detonation velocities, the jet axis is predicted to be liquid. This is coincident with copper material that is faster along the axis and leads the jet tip, forming a proboscis. At slower velocities this phenomena vanishes and the jet appears to be a solid.					
<b>15. SUBJECT TERMS</b> ALEGRA, shaped charge jet, velocity, temperature, explosive					
<b>16. SECURITY CLASSIFICATION OF:</b>			<b>17. LIMITATION OF ABSTRACT</b> UU	<b>18. NUMBER OF PAGES</b> 22	<b>19a. NAME OF RESPONSIBLE PERSON</b> Robert L Doney
<b>a. REPORT</b> Unclassified	<b>b. ABSTRACT</b> Unclassified	<b>c. THIS PAGE</b> Unclassified			<b>19b. TELEPHONE NUMBER (Include area code)</b> 410-278-7309

## **Contents**

---

---

<b>List of Figures</b>	<b>iv</b>
<b>List of Tables</b>	<b>iv</b>
<b>Acknowledgments</b>	<b>v</b>
<b>1. Introduction</b>	<b>1</b>
<b>2. Results and Discussion</b>	<b>2</b>
<b>3. Conclusion</b>	<b>9</b>
<b>4. References</b>	<b>10</b>
<b>Appendix. Temperature Profiles of Jet Tips</b>	<b>12</b>
<b>Distribution List</b>	<b>14</b>

## List of Figures

---

---

Fig. 1	Experimental X-ray flash of a 65-mm shaped charge jet at $45 \mu\text{s}$ .....	2
Fig. 2	Temperature (left) and melt (right) profiles .....	3
Fig. 3	Velocity profiles for jet segments exceeding 6 km/s .....	5
Fig. 4	Location for sampling the radial temperature profiles in jet tips .....	6
Fig. 5	(left) Temperature as a function of radial position for detonation velocities and sample times listed in Table 1, and (right) interpolated expression for temperature as a function of radial position .....	7
Fig. 6	Radial temperature profile for differing axial positions (velocities) and detonation velocities, $v_d$ .....	8
Fig. A-1	Temperature profiles and detonation velocity for jet tips .....	13

## List of Tables

---

---

Table 1	Explosive fills and detonation velocities .....	2
---------	---	---

## Acknowledgments

---

I am indebted to Drs Michael Zellner and Matthew Coppinger for their technical review of this work, and to Ms Nancy Simini for her careful editorial review. This work was supported in part by a grant of computer time from the DoD High Performance Computing Modernization Program at the Army Research Laboratory DoD Supercomputing Resource Center and the Terminal Ballistics Frontier project. I would also like to thank Dr Stephen Segletes and Mr Stephen Schraml for L<sup>A</sup>T<sub>E</sub>Xsupport.

## 1. Introduction

---

In advancing the field of terminal ballistics, it is helpful to understand the effects of a warhead's detonation velocity on the resulting speed and thermodynamic state of shaped charge jets. Historically, jet speed and state has been investigated in simulations (and experiments) by placing a conditioning plate of varying thickness at some point near the warhead to erode a certain amount of jet tip such that a lower velocity remains. However, this method creates additional debris that can affect certain types of armor simulations. Another approach in simulations is to delete material. While also successful for solid dynamics-based calculations, the thermodynamic state for each of these approaches remains that of a faster jet, rather than one generated under lower pressures. As such, temperatures may be inaccurately higher, which can affect other important jet properties as well.

The current work extends our recent 2D simulation-based thermodynamic characterization of jets.<sup>1</sup> Previously, we demonstrated good agreement with experiment for the jet's state when using an LX-14 explosive fill (detonation velocity,  $v_d = 8.8$  km/s) and resolution of 5 cells/mm. Specifically, we found that the 3337 SESAME<sup>2</sup> copper equation of state (EOS) and Steinberg-Guinan-Lund (SGL) models<sup>3,4</sup> generate results matching experiment in terms of jet tip speed and morphology,<sup>5</sup> bulk jet tip temperature,<sup>6</sup> and evidence of melt along the jet axis.<sup>7</sup> The new 3337 EOS<sup>8</sup> "has been compared to numerous data sets examining the behavior of the EOS both in expansion and compression and found to be in excellent agreement. Additionally, the new equation of state is superior to the previous SESAME equation of state 3336, in thermal expansion, heat capacity, and treatment of the melt. In all other comparisons, the two equations of state are comparable."

In this report, I use a 65-mm, bare, shaped charge jet, generated from explosives that feature detonation velocities ranging from 6.84 to 9.11 km/s. In all cases, the geometry remains fixed. Figure 1 displays a typical radiographic flash of a 65-mm shaped charge jet<sup>5</sup> at  $45 \mu s$ .

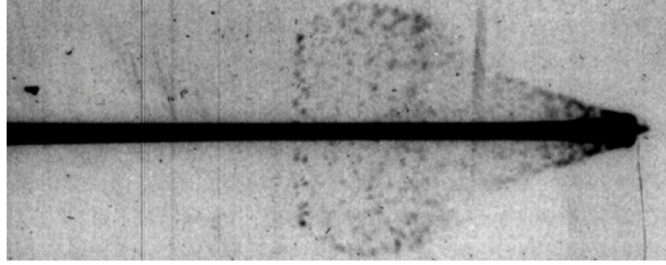


**Fig. 1** Experimental X-ray flash of a 65-mm shaped charge jet<sup>5</sup> at 45  $\mu$ s

Calculations are performed using Sandia National Laboratories' multiphysics code, ALEGRA<sup>9</sup> v.7.7. Again, the shaped charge jet is modeled with the 3337 copper EOS and SGL strength model. In all cases, explosives use the Jones-Wilkins-Lee<sup>10</sup> EOS with default detonation velocities. Simulations are run with a dry air background using SESAME 5030.

## 2. Results and Discussion

Table 1 lists the explosive models used, their default detonation velocities  $v_d$ , and data sample times (used in later figures). LX-14 is emphasized since it is a commonly used baseline.

**Table 1** Explosive fills and detonation velocities

Explosive	Detonation velocity, $v_d$ (km/s)	Sample time ( $\mu$ s)
HMX	9.11	37
<b>LX-14</b>	<b>8.8</b>	<b>37</b>
PETN4	8.3	37
PBX-9407	7.91	37
PBX-9502	7.71	37
PENTOLITE50/50	7.53	38
PENTOLITE	7.36	38
EL-506AA	7.2	39
EL-506CA	7.0	39
LX-01A	6.84	40

Figure 2 illustrates the predicted temperature profile (left) and liquid phase (right) for jets as a function of detonation velocity. For slower detonation velocities ( $v_d <$

7.71 km/s), I allowed the jet to evolve another 1-2  $\mu$ s to capture enough of the neck during visualization. This had no discernible effect on the results. Additionally, jets were translated in order to align tip positions. An expanded view of temperature profiles is illustrated in the Appendix.

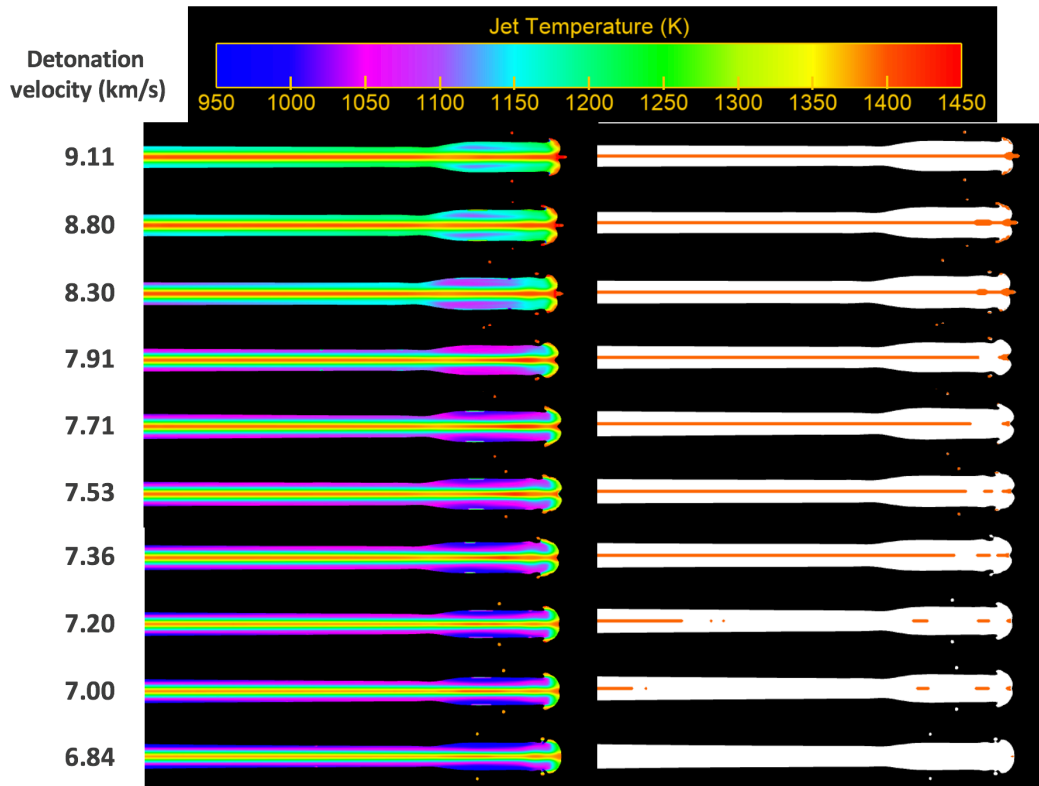


**Fig. 2** Temperature (left) and melt (right) profiles

Simulations indicate that the temperature distribution near jet tip surfaces changes considerably with detonation velocity. Here, the tip is defined as the region with larger radius. At high  $v_d$ , temperatures exceeding 1100 K are common. Below  $v_d = 8.3$  km/s, the spatial extent of temperatures below 1100 K increases. In all cases, the temperature along the axis is much higher than the surrounding regions—suggesting copper material along the axis may be melted (recall its ambient melt temperature is about 1358 K). Jet formation, however, creates density extremes,<sup>1</sup> so the SGL model is particularly appropriate since it has a density-dependent (Lindemann<sup>11,12</sup>) melt curve and the jet axis consists of densities smaller than ambient copper.

I use ALEGRA’s “phase control” capability which turns off the strength model when a material melts or vaporizes. It also offers new variables to inspect material phase—in our case, locations where copper may be liquid. The right-hand side of Fig. 2 plots the liquid copper isovolume (orange) over jet material (white). A continuous melt region along the axis is visible for jets with  $v_d > 7.91$  km/s. This may be why we see a proboscis similar to the experiment in Fig. 1. In the LX-14 simulation, we found that the proboscis begins to lead the jet after about 30  $\mu$ s (not pictured).

Currently, SGL is the only strength model that captures this seemingly correct temperature and melt state of jets.<sup>1</sup> We found that this is due to SGL’s pressure-dependent yield strength. If the pressure-dependence is turned off or another strength model is used, the phase change vanishes and all jet material becomes solid. This was only evaluated for LX-14; however, it is unlikely that smaller  $v_d$  would produce higher temperatures leading to a phase change. Additionally, the default melt temperature for copper in the SGL model—along with other metals—is higher, about 1790 K. This is due to volume change with increasing temperature, consistent with a density-dependent melt, inherited from SGL’s predecessor, GRAY (a three-phase EOS for metals).<sup>13</sup>

Below  $v_d = 8.3$  km/s, the melt continuity begins to break up inside the tip. This is coincident with the proboscis’ disappearance. Below  $v_d = 7.36$  km/s, the melt region is substantially reduced and by  $v_d = 6.84$  km/s, the jet tip and trailing neck appears as solid copper.

Figure 3 illustrates jet velocities as a function of  $v_d$ . Only portions of the jet exceed-

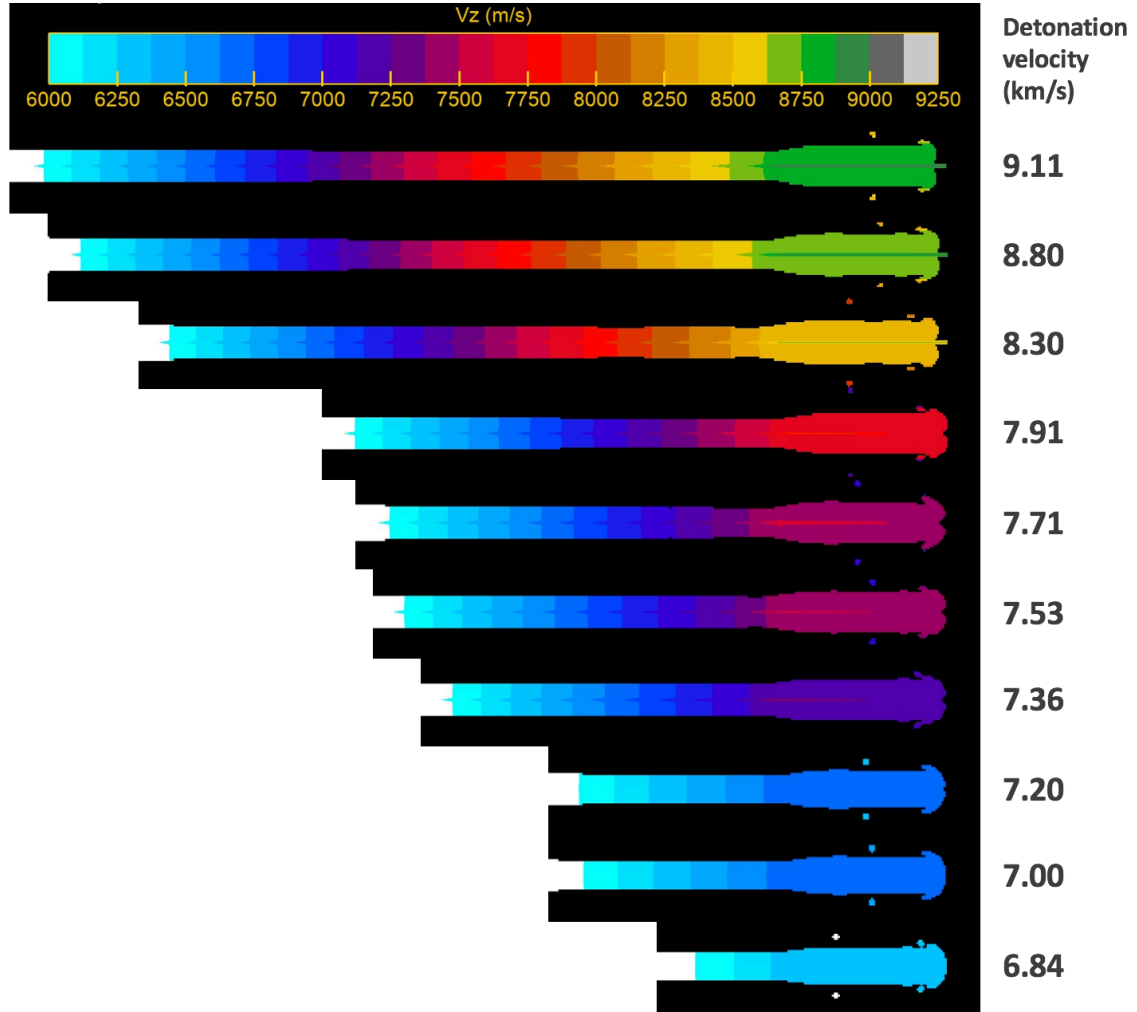


**Fig. 3 Velocity profiles for jet segments exceeding 6 km/s**

ing 6 km/s are shown. The data show that higher  $v_d$  leads to larger jet velocities. For  $v_d > 7.2$  km/s, regions near the axis appear to be 125–250 m/s faster. Again, this is coincident with the threshold for a liquid axis from Fig. 2. Along the jet neck, the left-pointing arrowheads are a result of higher axial velocities. In the  $v_d = 9.11$  km/s case, for example, the axial velocity,  $V_z = 6000$ – $6125$  m/s block (left-most, light blue), has a slightly faster speed of  $6125$ – $6250$  m/s along its faster section of the axis. This is true for all faster sections of the jets down through  $v_d = 7.36$  km/s—except for the jet tips with  $v_d < 8.3$  km/s.

Figure 4 illustrates the approximate location for sampling radial temperature profiles in jet tips. The position was selected for consistency—to be approximately

half-way along the jet tip and away from any interfering fragments.

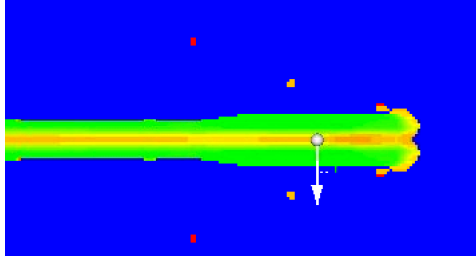


**Fig. 4 Location for sampling the radial temperature profiles in jet tips**

Using the approximate sampling location from Fig. 4, Fig. 5 (left panel) illustrates the temperature as a function of radial position for the various detonation velocities (also listed in Table 1). In most cases, the temperatures converge to about 1400 K at the axis. With increasing radii, temperatures decrease and diverge among the differing  $v_d$ , where smaller  $v_d$  leads to lower temperatures. The differing melt conditions along jet axes, despite similar axial temperatures, are likely due to the differences in pressure-driven densities early in the jets' formation—since density influences melt temperature.

The overall trend for differing  $v_d$  is similar enough to form a general expression for jet tip temperature as a function of radial position. Shown in Fig. 5 (right panel) are the sample points from Fig. 5 (left panel) and a second-order polynomial interpolant. This work finds that the jet tip temperature decreases with radius as

$$T = 141.6r^2 - 460.1r + 1419; \quad (r \leq 1.6) \quad , \quad (1)$$

where the radius,  $r$ , is in units of millimeters and temperature,  $T$ , is in Kelvin.

We can extend our analysis to look at radial temperature distributions of the jet necks—the elongating section behind the tip. Recalling the velocity profiles in Fig. 3, we can radially sample the temperature (as performed in Fig. 4) at different axial positions (i.e.,  $V_z = \{6.0, 6.5, \dots, 8.5\} \pm 0.05$  km/s for jets generated by different explosives and detonation velocities). These results are detailed in Fig. 6.

As Fig. 3 illustrates,  $v_d \propto V_z$ , so there are fewer velocity profiles visible in Fig. 6 with decreasing  $v_d$ . The cases are surprisingly similar and show a hot jet axis of about 1400 K that slowly decreases to about 1375 K as  $v_d$  gets smaller. We also

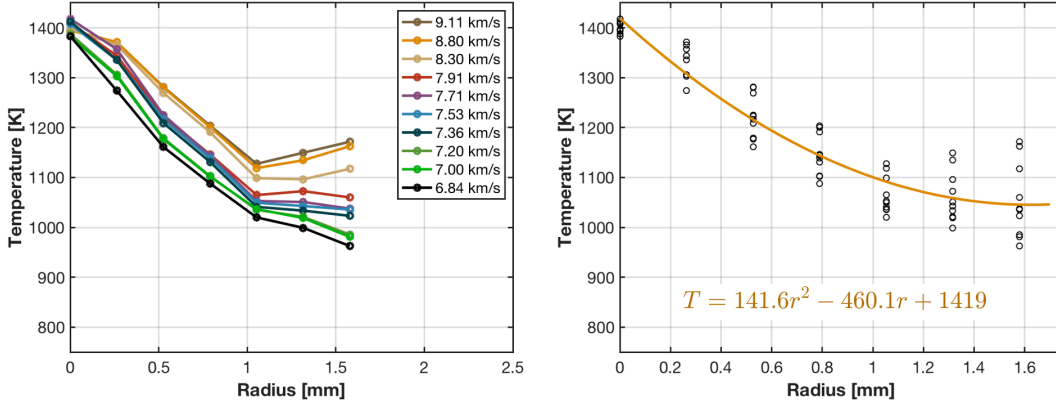


**Fig. 5 (left) Temperature as a function of radial position for detonation velocities and sample times listed in Table 1, and (right) interpolated expression for temperature as a function of radial position**

see that, in all cases, as we move toward the front of the jet (i.e., larger  $V_z$ ), we see higher temperatures at the jets' surfaces. In all cases, the temperature roughly decreases similarly along the neck of the jet. At higher  $v_d$ , differences emerge at about  $r = 0.75$  mm. This similarity increases to about  $r = 1$  mm for  $v_d \leq 7.71$  km/s. These temperature profiles are remarkably similar: minimum and maximum detonation velocities indicate that, at  $r \sim 1.25$  mm, the surface temperature only differs by approximately 25–50 K.

Interestingly, there does not appear to be a notable difference in the temperature profiles between  $v_d = 7.36$  and 7.2 km/s, as we saw in Figs. 2 and 3, which show a change in the prediction of liquid along the jets' axes.

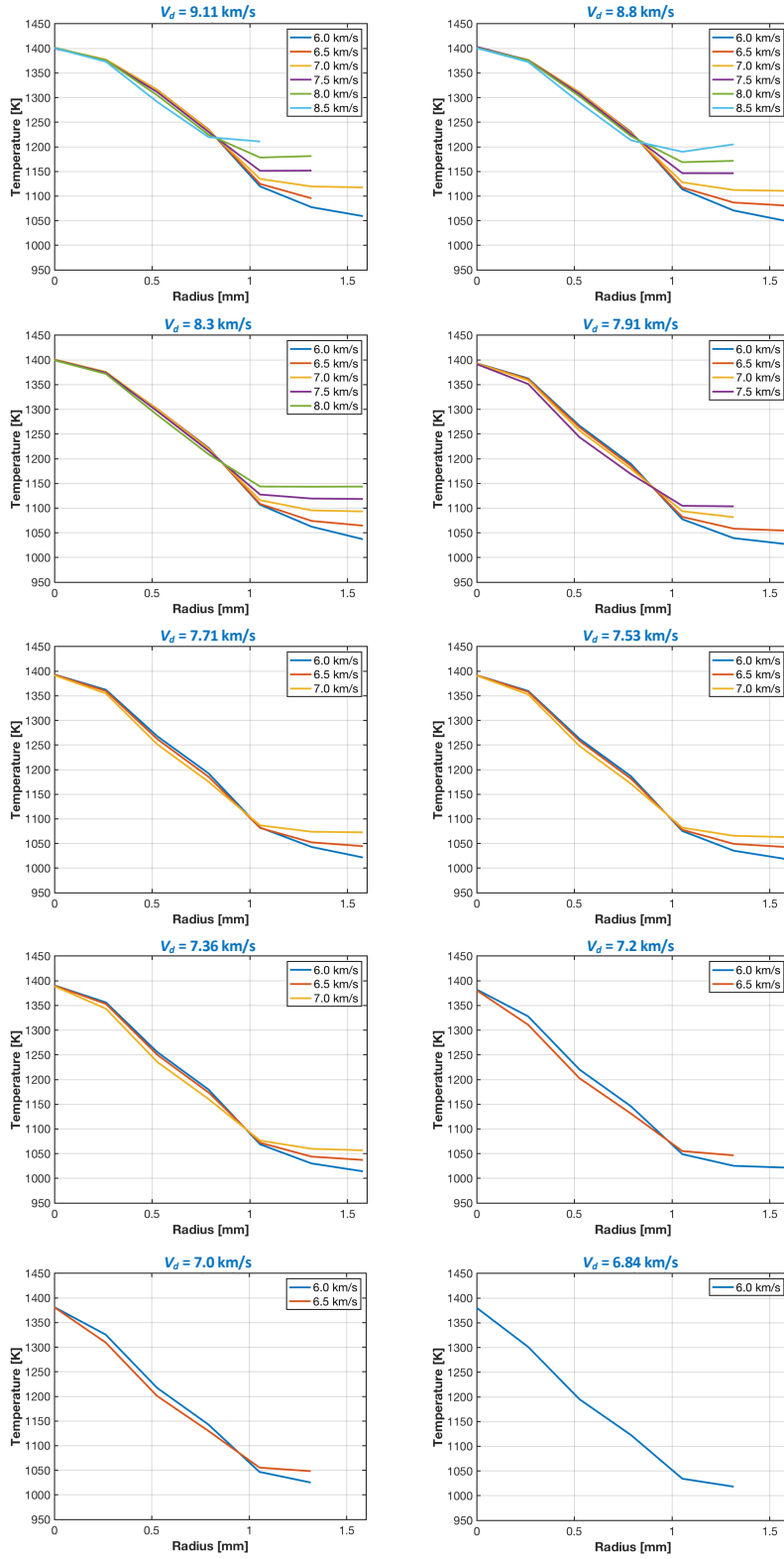


**Fig. 6** Radial temperature profile for differing axial positions (velocities) and detonation velocities,  $v_d$

### 3. Conclusion

---

In this report, I evaluated the effects of a warhead's detonation velocity on the resulting speed and thermodynamic state of shaped charge jets using the multiphysics code ALEGRA. Specifically, I investigate a 65-mm, bare, shaped charge jet, generated from explosives that feature detonation velocities ranging from 6.84 km/s to 9.11 km/s with a fixed geometry. Data for all jet tips showed a general trend: a hot axis that cools off with increasing radius according to a second-order polynomial. At higher detonation velocities, the jet axis is predicted to be liquid. This is coincident with copper material that is faster along the axis and leads the jet tip, forming a proboscis. At slower velocities this phenomena vanishes and the jet appears to be a solid.

Radial temperature profiles along the necks of these simulated jets were surprisingly similar. Profiles indicate a hot axis (about 1400 K) that decreased several hundred Kelvin with increasing radius. Temperature differences in any specific jet manifested mostly at the jet surface, where higher axial velocities (i.e., a position closer to the jet tip) lead to higher surface temperatures.

## 4. References

---

1. Doney R, Niederhaus JH, Fuller T, Coppinger M. Effects of equations of state and constitutive models on simulating copper shaped charge jets in ALEGRA. *International Journal of Impact Engineering*. 2020;136:103428.
2. McHardy JD. An introduction to the theory and use of SESAME equations of state. Los Alamos (NM): Los Alamos National Laboratory; 2018 Dec. Report No.: LA-14503.
3. Steinberg D, Cochran S, Guinan M. A constitutive model for metals applicable at high-strain rate. *Journal of Applied Physics*. 1980;51:1498.
4. Steinberg D, Lund C. A constitutive model for strain rates from  $10^{-4}$  to  $10^6 \text{ s}^{-1}$ . *Journal of Applied Physics*. 1998;65:1528.
5. Zellner MB, Vunni GB. Photon dopper velocimetry characterization of shaped charge jet formation. Aberdeen Proving Ground (MD): Army Research Laboratory (US); 2012 Apr. Report No.: ARL-TR-5961.
6. Uhlig WC, Hummer CR. In-flight measurement of shaped charge jet conductivity and temperature. Aberdeen Proving Ground (MD): Army Research Laboratory (US); 2011 July. Report No.: ARL-TR-5609.
7. Lassila D, Walters W, Nikkel D, Kershaw D. Evidence of melt in ‘soft’ recovered copper jets. Livermore (CA): Lawrence Livermore National Laboratory; 1995 Aug. Report No.: UCRL-JC-120717.
8. Peterson J, Honnell K, Greeff C, Johnson J, Boettger J, Crockett S. Global equation of state for copper. Los Alamos (NM): Los Alamos National Laboratory; 2011. Report No.: LA-UR-11-04443.
9. Robinson A, Brunner T, Carroll S, Drake R, Garasi C, Gardiner T, Hail T, Hanshaw H, Hensinger D, Labreche D, et al. ALEGRA: An arbitrary Lagrangian-Eulerian multimaterial, multi-physics code. In: *Proceedings of the 46th AIAA Aerospace Sciences Meeting*. 2008 Jan 7–10; Reno, NV. Paper No.: AIAA-2008-1235.
10. Kerley GI. CTH reference manual: the equation of state package. Albuquerque (NM): Sandia National Laboratories; 1998. Report No.: SAND98-0947.

11. Lindemann FA. Phys. Z. 1910;11:609.
12. Stacey FD, Irvine RD. Theory of melting: thermodynamic basis of Lindemann's Law. Australian Journal of Physics. 1977;30:631–640.
13. Royce EB. GRAY, a three-phase equation of state for metals. Livermore (CA): Lawrence Livermore Laboratory; 1971 Sep. Report No.: UCRL-51121.

## **Appendix. Temperature Profiles of Jet Tips**

---

---

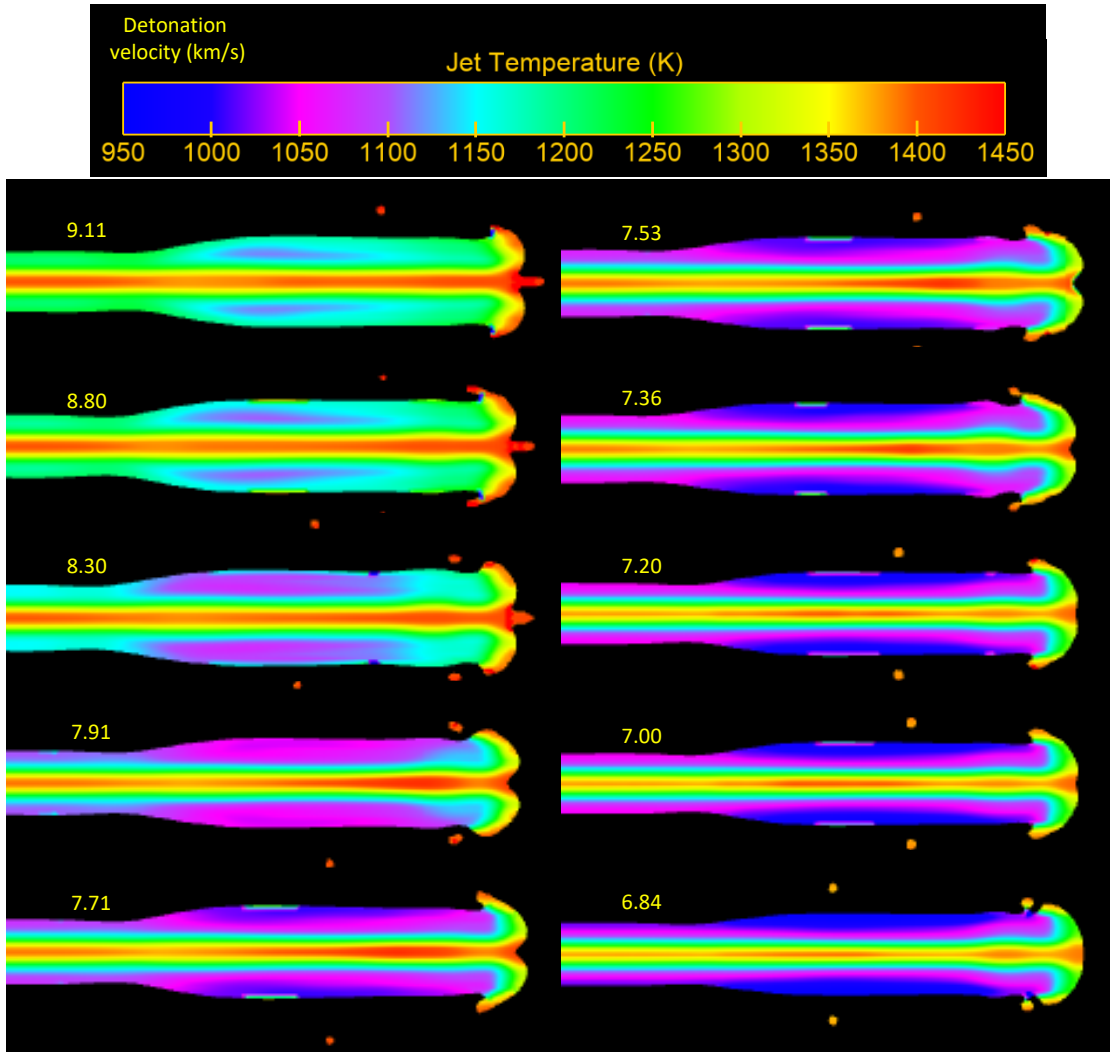


Fig. A-1 Temperature profiles and detonation velocity for jet tips

1 DEFENSE TECHNICAL  
(PDF) INFORMATION CTR  
DTIC OCA

1 CCDC ARL  
(PDF) FCDD RLD CL  
TECH LIB

1 AFRL  
(PDF) K VANDEN

1 CCDC ARMAMENTS CENTER  
(PDF) K MIERS  
S DEFISHER

1 CCDC GVSC  
(PDF) F RICKERT

1 DSTO - AUSTRALIA  
(PDF) S RYAN

2 FOI - SWEDEN  
(PDF) P APPELGREN  
P LUNDBERG

2 IDAHO NATIONAL LABORATORY  
(PDF) B AYDELOTTE  
J LACY

1 LOS ALAMOS NATIONAL LABORA-  
(PDF) TORY  
M BURKETT

2 NAVSEA DAHLGREN  
(PDF) C DYKA  
M HOPSON

1 PD MBTS  
(PDF) E BARSHAW

9 SANDIA NATIONAL LABORATORIES  
(PDF) S BOVA  
J CARPENTER  
K COCHRANE  
D DEDERMAN  
J KORBIN  
J NIEDERHAUS  
A RODRIGUEZ  
A SOKOLOW  
J WILKES

ABERDEEN PROVING GROUND

S KUKUCK  
J STEWART

44  
(PDF)

DIR CCDC ARL

FCDD-RLW-LH

E KENNEDY

J O'GRADY

C MEYER

M MINNICINO

D SCHEFFLER

B SORENSEN

R SUMMERS

M WALTER

FCDD-RLW-MB

Z WILSON

FCDD-RLW-PA

P BERNING

S BILYK

M COPPINGER

C UHLIG

FCDD-RLW-PC

R BECKER

J CAZAMIAS

M GRINFELD

B LEAVY

C MEREDITH

J LLOYD

S SEGLETES

C WILLIAMS

FCDD-RLW-PD

A BARD

W CLARK

R DONEY

S HALSEY

M KEELE

D KLEPONIS

B KRZEWINSKI

K MASSER

R MUDD

F MURPHY

C RANDOW

S SCHRAML

G VUNNI

M ZELLNER

FCDD-RLW-PE

D GALLARDY

D HORNBAKER

J HOUSKAMP

E KLIER

C KRAUTHAUSER

M LOVE

P SWOBODA

FCDD-RLW-PG